DOI 10.5012/bkcs.2010.31.01.120

Effect of Bimetallic Pt-Rh and Trimetallic Pt-Pd-Rh Catalysts for Low Temperature Catalytic Combustion of Methane

Margandan Bhagiyalakshmi, Ramani Anuradha, Sang Do Park,† Tae Sung Park,† Wang Seog Cha,‡ and Hyun Tae Jang*

*Chemical Engineering Department, Hanseo University, Seosan 360-706, Korea. *E-mail: htjang@hanseo.ac.kr*
†Carbon Dioxide Reduction & Sequestration Research Center, Korea Institute of Energy Research, Deajeon 305-343, Korea
‡School of Civil and Environ., Kunsan National University, Kunsan, Jeonbuk 573-701, Korea
Received July 16, 2009, Accepted November 11, 2009

Monometallic, bimetallic and trimetallic particles consisting of different weight compositions of Pt-Pd-Rh over pure alumina wash coats have been synthesized and their catalytic performance on methane conversion was studied from 150 to 600 °C. Different catalyst formulations with variable Pt, Pd and Rh contents for bimetallic and trimetallic systems were tried and $Pt_{(1.5)}Rh_{(0.3)}/Al_2O_3$ and $Pt_{(1.0)}Pd_{(1.0)}Rh_{(0.3)}/Al_2O_3$ shows low T_{50} and T_{90} temperatures. Bimetallic and trimetallic particle synergism acts as three way catalysts and therefore, all the catalysts show 100% methane conversion. The effect of supports such as ZrO_2 and TiO_2 on methane combustion was investigated; from T_{50} and T_{90} results both Al_2O_3 and ZrO_2 are suitable supports for low temperature methane combustion.

Key Words: Methane conversion, Bimetallic, Trimetallic, Pt-Rh/Al_2O_3, Pt-Rh/ZrO_2

Introduction

Catalytic combustion of methane attracts researcher's attention due to the quest against lowering of combustion temperature, negligible contribution of NO_x, and CO or particulate matter to the atmosphere. Many reports on noble metal catalysts for complete combustion of hydrocarbons are available.[1-4] Among the noble-metal catalysts, palladium and platinum on various wash coats have been reported as the most active catalysts for methane combustion, due to their high thermal stability, but easily deactivated by sulphur poison.[5-11] Recent reports portray that bimetallic catalysts exhibit better properties like improved activity, selectivity, and thermal stability than monometallic catalysts. Many reports revealed the improved activity of Pt-Pd bimetallic catalysts over monometallic Pd catalysts,[12-14] as metal-metal interactions are believed to overcome deactivation of catalysts with time on stream.

Furthermore, the performance of Pt-Rh bimetallic catalysts was promising in reported[16,17] synergistic adsorption of NO_x, during the production of thermal energy by methane combustion.[15] The effect of bimetallic Pt-Rh alloy formation depicts that Pt oxidizes hydrocarbons and byproducts, formed during combustion while rhodium reduces nitric oxides to nitrogen. Therefore, in our study, we synthesized bimetallic Pt-Rh and trimetallic Pt-Rh-Pd catalyst and investigated methane combustion. Previous reports on bimetallic alloy,[18,19] rendered that the metal composition as well as the metal-support interaction influence alloy formation which perhaps alters the catalytic activity.[20] Taking this into account, we tried various combinations of noble metal composition to obtain binary and ternary alloys of Pt, Rh and Pd on different supports for methane combustion. The effect of catalytic supports such as Al_2O_3, TiO_2 and ZrO_2 in alloy formation and its impact on combustion was also explored. These binary and ternary noble metal catalysts facilitate low temperature methane combustion analogous to well established methane combustion catalysts.

Experimental

High purity $H_2PtCl_6{\cdot}6H_2O$, $PdCl_2$, and $RhCl_3{\cdot}xH_2O$, supplied from Aldrich Co., were used as precursors for Pt-Pd-Rh/Al_2O_3 catalysts. The wash coats of Pt, Pt-Rh and Pt-Rh-Pd catalysts supported on γ-alumina (Surface area: 155 m^2/g, 58 Å, ~155 mesh, Aldrich Chem. Co.), ZrO_2 and TiO_2 with various weight percentage loadings were synthesized by the following method. 0.2 M HCl solution was added to the support (γ-alumina) before impregnating the noble metal salts in order to introduce chloride as competing ion for homogeneous distribution of metal ions. The solution of metal salts was impregnated on alumina and the mixture was evaporated in the rotary evaporator at 70 °C to remove excess water. Thereafter the material obtained was dried at 110 °C at 12 h and calcined in air (60 mL min^{-1}, 4 h, 450 °C), flushed with N_2 for 30 min and then reduced with flowing H_2 (60 mL min^{-1}, 4 h, 500 °C).[21] The catalysts obtained were denoted as $Pt_xRh_yPd_z/Al_2O_3$, $Pt_xRh_yPd_z/ZrO_2$, $Pt_xRh_yPd_z/TiO_2$, where x, y and z are weight percentages of respective metals.

Powder X-ray diffraction patterns were recorded using a Rigaku Miniflex diffractometer with Cu-Kα radiation (λ = 1.54 Å) in the 2 θ range 10 - 70° at 0.02 step size and 1 s step time. The surface morphologies of the catalyst were examined by Scanning Electron Microscopy (SEM) after gold coating using a FEI Quanta 200 instrument operating at 30 keV and equipped with an Energy-dispersive X-ray spectroscopy (EDAX). Temperature Programmed Reduction (TPR) assays were performed in an AutoChem II 2920 (Micromeritics). Initially all the samples are oxidized at 600 °C with 2% O_2 in argon mixture. Thereafter, the oxidized samples were reduced using 4.8% hydrogen in argon flow at a heating rate of 10 °C /min and a gas flow rate of 15 mL/min.

Catalytic activity was evaluated on a homemade quartz fixed-bed reactor (i.d. = 8 mm) with 0.1 mL catalyst (40 - 60 mesh) at atmospheric pressure (Fig. 1). The reactant mixture

Table 1. T_{50} and T_{90} temperature for methane conversion over bi and trimetallic catalysts

Catalyst	CH_4 Conversion	
	T_{50} (°C)	T_{90} (°C)
$Pt_{(1.0)}/Al_2O_3$	474	520
$Pt_{(0.25)}Rh_{(0.0375)}/Al_2O_3$	495	530
$Pt_{(0.5)}Rh_{(0.075)}/Al_2O_3$	480	522
$Pt_{(0.5)}Rh_{(0.15)}/Al_2O_3$	445	475
$Pt_{(0.75)}Rh_{(0.15)}/Al_2O_3$	433	470
$Pt_{(1.5)}Rh_{(0.3)}/Al_2O_3$	415	460
$Pt_{(1.5)}Rh_{(0.3)}/TiO_2$	458	480
$Pt_{(1.5)}Rh_{(0.3)}/ZrO_2$	425	475
$Pt_{(0.25)}Pd_{(0.25)}Rh_{(0.075)}/Al_2O_3$	488	520
$Pt_{(0.5)}Pd_{(0.5)}Rh_{(0.15)}/Al_2O_3$	465	495
$Pt_{(1.0)}Pd_{(1.0)}Rh_{(0.3)}/Al_2O_3$	430	468
$Pt_{(1.0)}Pd_{(0.75)}Rh_{(0.25)}/Al_2O_3$	388	442
$Pt_{(1.0)}Pd_{(0.75)}Rh_{(0.25)}/TiO_2$	465	496
$Pt_{(1.0)}Pd_{(0.75)}Rh_{(0.25)}/ZrO_2$	436	442

(0.1% CH_4 + 16.74% O_2 + 83.16% N_2) was passed over pre-activated catalysts at space velocity 10,000 h^{-1} and methane combustion was studied between 150 °C and 600 °C in step of 30 °C. The combustion products were analyzed using on-line Gas Chromatography (GC) (Agilent series 6890 N) equipped with HP 6890n (30 m) column, using He as the carrier gas. Methane conversion data was calculated by the difference between inlet and outlet concentrations using Flame Ionization Detector (FID), while the byproducts, Hydrogen and CO_2 were detected through Thermal conductivity Detector (TCD). No CO_2 or hydrogen was observed, implies complete conversion of methane and its % conversion was calculated using the formula

$$\% \text{ Conversion} = \frac{[\text{Initial methane concentration} - \text{Final methane concentration}] \times 100}{\text{Initial methane concentration}}$$

The breakthrough plots of methane conversion Vs temperature for all the catalysts, illustrate T_{50} and T_{90} for methane conversion.

Result and Discussion

The XRD patterns of reduced bimetallic Pt-Rh and trimetallic Pt-Rh-Pd catalysts, at high and low metal compositions are shown in Fig. 2 Peaks due to Pt, Rh and Pd are let undetected against reflections from alumina, indicating tiny metallic particles on the alumina surface, which are difficult to estimate through XRD[22,23] even at high metal compositions ($Pt_{(1.0)}Pd_{(1.0)}Rh_{(0.3)}/Al_2O_3$). Therefore, complete interpretation of bi or trimetallic nature by XRD is unfeasible.

Fig. 3 displays the SEM images of $Pt_{(0.25)}Pd_{(0.25)}Rh_{(0.075)}/Al_2O_3$ and $Pt_{(1.0)}Pd_{(1.0)}Rh_{(0.3)}/Al_2O_3$ catalysts and the EDAX

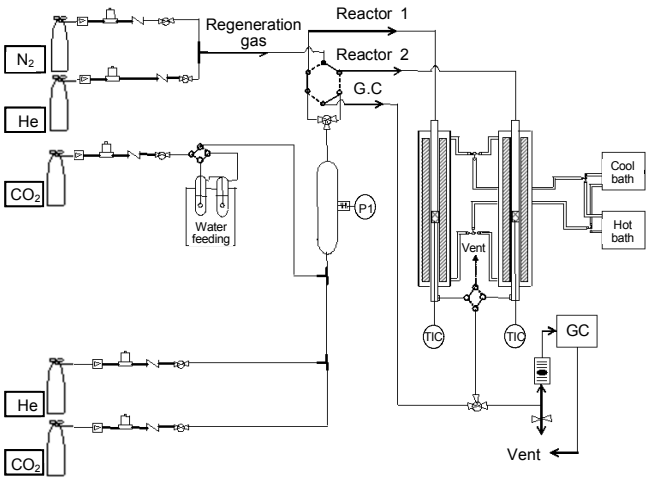

Figure 1. Schematic of the home-made fixed bed reactor for methane combustion.

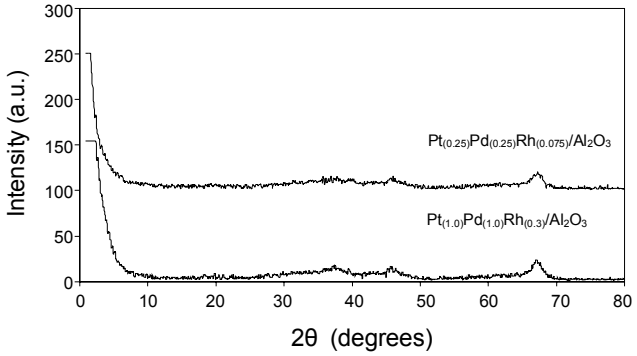

Figure 2. XRD patterns of (A) $Pt_{(0.25)}Pd_{(0.25)}Rh_{(0.075)}/Al_2O_3$, (B) $Pt_{(1.0)}Pd_{(1.0)}Rh_{(0.3)}/Al_2O_3$ catalysts.

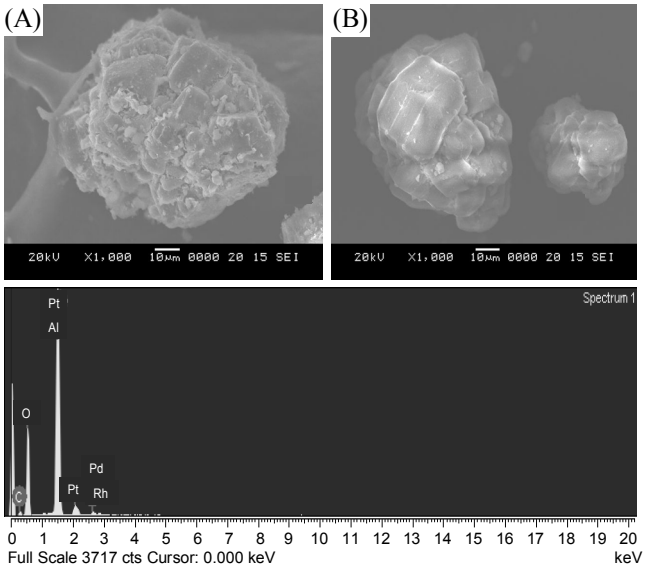

Figure 3. SEM images of (A) $Pt_{(0.25)}Pd_{(0.25)}Rh_{(0.075)}/Al_2O_3$, (B) $Pt_{(1.0)}Pd_{(1.0)}Rh_{(0.3)}/Al_2O_3$ catalysts and Energy dispersive X-ray spectroscopy measurements for $Pt_{(1.0)}Pd_{(1.0)}Rh_{(0.3)}/Al_2O_3$.

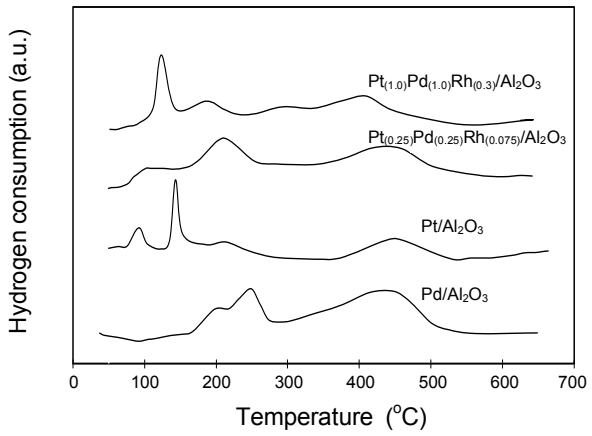

Figure 4. TPR results of (A) $Pt_{(1.0)}/Al_2O_3$, (B) $Pd_{(1.0)}/Al_2O_3$, (C) $Pt_{(0.25)}Pd_{(0.25)}Rh_{(0.075)}/Al_2O_3$, (D) $Pt_{(1.0)}Pd_{(1.0)}Rh_{(0.3)}/Al_2O_3$ catalysts.

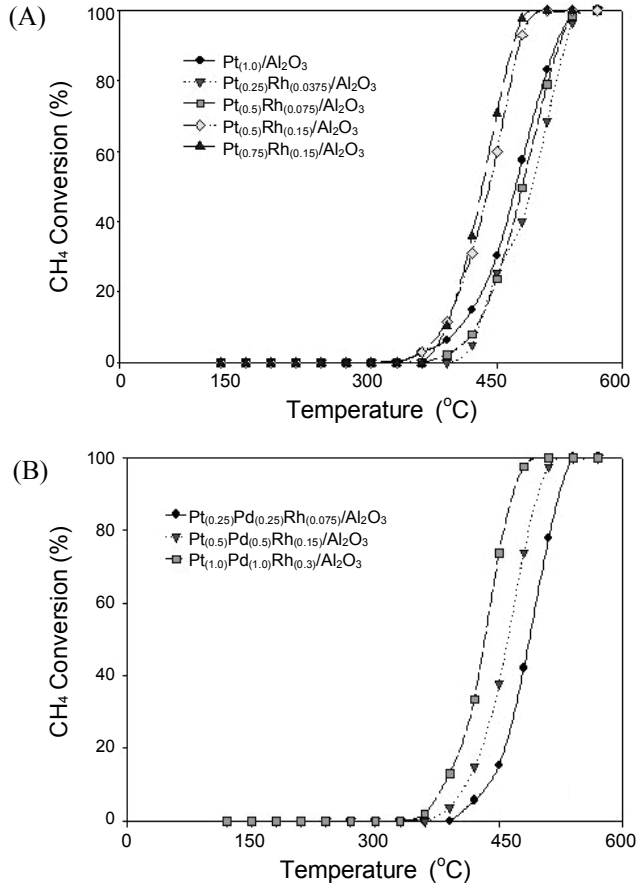

Figure 5. Methane conversion over (A) bimetallic catalysts and (B) trimetallic catalysts.

analysis for $Pt_{(1.0)}Pd_{(1.0)}Rh_{(0.3)}/Al_2O_3$. SEM as well EDAX results show no distinct metal particles, which clearly confirm well dispersion of metal particles over alumina surface. Only at high composition $Pt_{(1.0)}Pd_{(1.0)}Rh_{(0.3)}/Al_2O_3$, the presence of Pt, Pd and Rh were observed from EDAX and the results are 0.92, 0.89 and 0.25 wt % respectively.

Fig. 4 shows the TPR profiles of $Pt_{(1.0)}/Al_2O_3$, $Pd_{(1.0)}/Al_2O_3$, $Pt_{(0.25)}Pd_{(0.25)}Rh_{(0.075)}/Al_2O_3$, and $Pt_{(1.0)}Pd_{(1.0)}Rh_{(0.3)}/Al_2O_3$ ca-

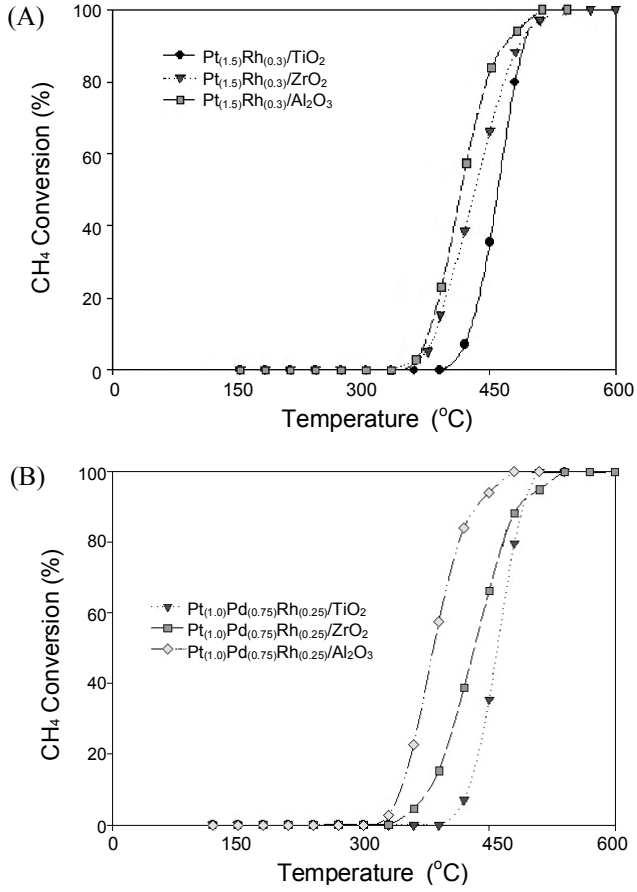

Figure 6. Effect of support on methane conversion (A) bimetallic catalysts and (B) trimetallic catalysts.

talysts. TPR results of monometallic Pd/Al_2O_3 and Pt/Al_2O_3 catalysts show two peaks, correspond to reduction of PdO around 140 °C and PtO around 250 °C. In the case of low and high composition trimetallic systems, shift in characteristic peaks due to monometallic Pt and Pd towards low temperature indicates high degree of interaction or metal alloying. Herein, Pd increased the reducibility of Pt particles, which might be due to spilt over H_2 from Pd particles to Pt and Rh particles. Similar phenomenon has been reported for Pt and Re catalysts in naphtha reforming.[24,25]

Methane combustion was carried out over Pt/Al_2O_3 and $Pt\text{-}Rh/Al_2O_3$, and the results are illustrated in Fig. 5A. From the results, $Pt_{(1.0)}/Al_2O_3$ catalyst shows 100% conversion, T_{50} and T_{90} are 472 °C and 523 °C respectively (Table 1). However, in the presence of Rh, conversion temperature either increases or decreases depending on its percentage composition in the bimetallic catalyst. Conversion temperature over $Pt_{(0.25)}/Rh_{(0.0375)}/Al_2O_3$ was observed to be higher than $Pt_{(1.0)}/Al_2O_3$. However, on increasing the composition of Pt and Rh, the conversion temperature decreased significantly compared to the monometallic catalyst. This observation suggests the formation of Pt-Rh bimetallic particles, which in turn enhances its activity for methane combustion. Hence it is concluded that the metal composition is the deciding factor for the formation of bimetallic particles as low composition $Pt_{(0.25)}Rh_{(0.0375)}/Al_2O_3$ ca-

talyst lacks alloying or metallic interactions to form bimetallic particle. Consequently, from this study, high composition Pt-Rh bimetallic catalysts favor low temperature methane conversion. Since, at low composition ($Pt_{(0.25)}Rh_{(0.0375)}/Al_2O_3$), bimetal formation was ignored due to well separated metal particles. From the Table 1, T_{50} and T_{90} temperatures for high composition catalysts ($Pt_{(0.5)}Rh_{(0.075)}/Al_2O_3$) is slightly less compared to low composition catalysts ($Pt_{(0.25)}Rh_{(0.0375)}/Al_2O_3$). In addition, on comparing various combinations of Pt and Rh, methane combustion results illustrate the similarity of $Pt_{(1.5)}Rh_{(0.3)}/Al_2O_3$ and $Pt_{(0.75)}Rh_{(0.15)}/Al_2O_3$ in relation to T_{50} and T_{90} conversion temperatures. Finally, the result focuses the betterment of bimetallic Pt-Rh catalyst than their monometallic-Pt counterparts for low temperature methane conversion. The synergism exerted on account of bimetallic Pt-Rh formation is similar with the already reported results.[18,20] As, all the catalysts exhibit 100% conversion between 400 and 550 °C, they may posses coke tolerance; even at low Pt-Rh composition, well-separated solo metallic particles also confer coke tolerance to the catalyst.

Composition dependence of trimetallic Pt-Pd-Rh/Al_2O_3 catalysts, also evidenced by decrease in T_{50} and T_{90} (Table 1) temperatures for methane conversion, is shown in Fig. 5B. For the $Pt_{(0.25)}Pd_{(0.25)}Rh_{(0.075)}/Al_2O_3$ catalysts methane conversion temperature is high, around 487 °C, in spite of 100% conversion. Hence, trimetallic particle formation is unfavorable similar to that of bimetallic particle on alumina at low compositions as discussed earlier. At high composition $Pt_{(0.5)}Pd_{(0.5)}Rh_{(0.15)}/Al_2O_3$ and $Pt_{(1.0)}Pd_{(1.0)}Rh_{(0.3)}/Al_2O_3$ catalysts, T_{50} temperatures are 465 and 430 °C respectively, which clearly depict the composition dependence even for ternary alloying. The observed decrease in conversion temperature than bimetallic Pt-Rh catalysts evidences the trimetallic Pt-Pd-Rh particle formation.

Fig. 6A shows the activity of Pt-Rh bimetal particles on other supports like TiO_2 and ZrO_2 for methane conversion. Pt-Rh/Al_2O_3 catalyst appears to be less active than Pt-Rh/ZrO_2. The decrease in combustion temperature to low values of the latter catalysts clearly evidences (Fig. 6A) distinct alloying of Pt and Rh facilitated by ZrO_2. The more Lewis acid property of ZrO_2 than Al_2O_3 might be the cause for adsorbing Pt and Rh precursors on its surface and their subsequent bimetal formation after reduction, which is supported by the pervious reports.[12] As ZrO_2 is less acidic than Al_2O_3,[26] thermal cracking reactions and coke formation are reduced.[27] Previous reports preferred ZrO_2 support for Rh catalysts, in order to avoid detrimental interaction between Rh and alumina (Al_2O_3), that reduces the activity of the catalyst.[28] However, the disadvantage of ZrO_2 is low surface area compared to other supports.[28] But TiO_2 with its bare outer surface and with less number of free defective hydroxyl groups might be inadequate to adsorb sufficient amount of Pt and Rh precursors to form bimetal particles and hence conversion is not exceeding 50%. Hence this study clearly demonstrates both Al_2O_3 and ZrO_2 are better supports than TiO_2. The ternary metal system also has similar effect over different supports in methane conversion and the results are shown in Table 2 and Fig. 6B.

The effect of space velocities on methane conversion (not shown) was also studied. It was observed that on increasing the space velocity beyond 30,000 h^{-1}, conversion slightly decreased due to less accessibility of methane gas on the active sites of the catalysts.

Conclusions

Wash coats of bimetallic Pt-Rh and trimetallic Pt-Rh-Pd on Al_2O_3, ZrO_2 and TiO_2 were synthesized and subjected to methane combustion. All the catalysts show 100% conversion of methane, and T_{50} and T_{90} temperatures were also noted. T_{50} and T_{90} temperature for the bimetallic and trimetallic catalysts depends on the composition of noble metals. $Pt_{(1.0)}Pd_{(1.0)}Rh_{(0.3)}/Al_2O_3$ catalysts with high Pd content showed low T_{50} and T_{90} temperatures, 430 and 468 °C respectively, for low temperature methane combustion, which exemplifies the dependency of Pd content on alloying. Among the supports studied, T_{50} and T_{90} temperatures on Al_2O_3 and ZrO_2 are low and hence both Al_2O_3 and ZrO_2 are suitable supports for methane combustion. Study of effect of space velocity substantiates the decrease in methane conversion beyond the space velocity of 30,000 h^{-1}.

Acknowledgments. The corresponding and the first authors thank the President of Hanseo University, for his constant help and openhanded opportunity to carry out this research.

References

1. Deutschmann, O.; Behrendt, F.; Warnatz, J. *Catal. Today* **1994**, *21*, 461.
2. Veser, G.; Frauhammer, J.; Schmidt, L. D.; Eigenberger, G. *Stud. Surf. Sci. Catal.* **1997**, *109*, 273.
3. Lapisardi, G.; Urfels, L.; Gélin, P.; Primet, M.; Kaddouri, A.; Garbowski, E.; Toppi, S.; Tena, E. *Catal. Today* **2006**, *117*, 564.
4. Bonarowska, M.; Karpiński, Z. *Catal. Today* **2008**, *137*, 498.
5. Choudhary, T. V.; Banerjee, S.; Choudhary, V. R. *Appl. Catal. A: Gen.* **2002**, *234*, 1.
6. Gélin, P.; Primet, M. *Appl. Catal. B: Environ.* **2002**, *39*, 1.
7. Gélin, P.; Urfels, L.; Primet, M.; Tena, E. *Catal. Today* **2003**, *83*, 45.
8. Burch, R.; Urbano, F. J. *Appl. Catal. A: Gen.* **1995**, *124*, 121.
9. Narui, K.; Yata, H.; Furuta, K.; Nishida, A.; Kohtoku, Y.; Matsuzaki, T. *Appl. Catal. A: Gen.* **1999**, *179*, 165.
10. Ersson, A.; Kusar, H.; Carroni, R.; Griffin, T.; Jaras, S. *Catal. Today* **2003**, *83*, 265.
11. Deng, Y.; Nevell, T. G. *Catal. Today* **1999**, *47*, 279.
12. Narui, K.; Yata, H.; Furuta, K.; Nishida, A.; Kohtoku, Y.; Matsuzaki, T. *Appl. Catal. A: Gen.* **1999**, *179*, 165.
13. Ozawa, Y.; Tochihara, Y.; Watanabe, A.; Nagai, M.; Omi, S. *Appl. Catal. A : Gen.* **2004**, *259*, 1.
14. Persson, K.; Ersson, A.; Jansson, K.; Iverlund, N.; Jaras, S. *J. Catal.* **2005**, *231*, 139.
15. Polvinen, R.; Vippola, M.; Valden, M.; Lepistö, T.; Suopanki, A.; Härkönen, M. *Surf. Interface Anal.* **2004**, *36*, 741.
16. Matsumoto, Y.; Okawa, Y.; Fujita, T.; Tanaka, K. I. *Surf. Sci.* **1996**, *355*, 109.
17. Nelson, A. E.; Schulz, K. H. *Appl. Surf. Sci.* **2003**, *210*, 206.
18. Kaila, R. K.; Gutiérrez, A.; Slioor, R.; Kemell, M.; Leskelä, M.; Outi, A.; Krause, I. *Appl. Catal. B: Environ.* **2008**, *84*, 223.
19. Souza, M. M. V. M.; Schmal, M. *Catal. Lett.* **2003**, *91*, 11.
20. Polvinen, R.; Vippola, M.; Valden, M.; Lepistö, T.; Suopanki, A.; Härkönen, M. *J. Catal.* **2004**, *226*, 372.
21. Mazzieri, V. A.; Grau, J. M.; Vera, C. R.; Yori, J. C.; Parera, J. M.; Pieck, C. L. *Catal. Today* **2005**, *107-108*, 643.

22. Garrigós-Pastor, G.; Parres-Esclapez, S.; Bueno-López, A.; Illán-Gómez, M. J.; Salinas-Martínez de Lecea, C. *Appl. Catal. A: Gen.* **2009**, *354*, 63.
23. Linjie, H.; Kenneth, A. B.; Josephine M. H. *J. Mol. Catal. A: Chem.* **2006**, *259*, 51.
24. Isaac, B. H.; Petersen, E. E. *J. Catal.* **1984**, *85*, 8.
25. Chen, L.; Li, Y.; Zang, J.; Luo, X.; Cheng, S. *J. Catal*. **1994**, *145*, 132.
26. Deng, Y.; Nevell, T. G. *Catal. Today* **1999**, *47*, 279.
27. Yamamoto, H.; Uchida, H. *Catal. Today* **1998**, *45*, 147.
28. Ersson, A.; Kusar, H.; Carroni, R.; Griffin, T.; Jaras, S. *Catal. Today* **2003**, *83*, 65.